arXiv:1208.0727v1 [hep-ph] 3 Aug 2012

Neutrinoless Double Beta Decay and Physics Beyond the Standard Model

Frank F. Deppisch[1*], Martin Hirsch[2†] and Heinrich Päs[3‡]

[1] *Department of Physics and Astronomy, University College London, UK*

[2] *AHEP Group, Instituto de Física Corpuscular, Universitat de Valencia, Spain*

[3] *Fakultät für Physik, Technische Universität Dortmund, Germany*

Abstract

Neutrinoless double beta decay is the most powerful tool to probe not only for Majorana neutrino masses but for lepton number violating physics in general. We discuss relations between lepton number violation, double beta decay and neutrino mass, review a general Lorentz invariant parametrization of the double beta decay rate, highlight a number of different new physics models showing how different mechanisms can trigger double beta decay, and finally discuss possibilities to discriminate and test these models and mechanisms in complementary experiments.

PACS numbers: 23.40.BW, 11.30.Fs 14.80

Keywords: Double beta decay, Lepton number violation, Physics beyond the Standard Model

1 Introduction

The search for neutrinoless double beta decay ($0\nu\beta\beta$) - the simultaneous transformation of two neutrons into two protons, two electrons and nothing else - is the most sensitive tool for probing Majorana neutrino masses (see the contribution by Rodejohann [1]). However, while this so-called mass mechanism is certainly the most prominent realization of the decay, and while an uncontroversial detection of neutrinoless double beta decay will inevitably guarantee that neutrinos are Majorana particles, Majorana neutrino masses are not the only element of beyond Standard Model physics which can induce double beta.

*E-mail: f.deppisch@ucl.ac.uk

†E-mail: mahirsch@ific.uv.es

‡E-mail: heinrich.paes@uni-dortmund.de

In this review we discuss mechanisms of neutrinoless double beta decay where the lepton number violation (LNV), necessary for the decay, does not directly originate from Majorana neutrino masses but rather due to lepton number violating masses or couplings of new particles appearing in various possible extensions of the Standard Model. While the same couplings will also induce Majorana neutrino masses, due to the Schechter-Valle black box theorem [2, 3], in these cases the double beta decay half life will not yield any *direct* information about the neutrino mass.

We start our review with a general consideration of black box contributions to neutrinoless double beta decay and neutrino masses. Next, we discuss a general framework which allows to parametrize and analyze any single contribution to neutrinoless double beta decay allowed by Lorentz invariance. While the neutrino mass limit is based on the well-known mechanism exchanging a massive Majorana neutrino between two standard model $(V-A)$ vertices, the effective vertices appearing in the new contributions involve non–standard currents such as scalar, pseudoscalar and tensor currents. Moreover, besides contributions with a light neutrino being exchanged between two separated vertices, the so-called long-range part, additional contributions from short range mechanisms are possible, where exchanged particles are all much heavier than the typical length scale of nuclear separation, such as in supersymmetry (SUSY) without R–parity. Then we turn to several concrete models such as left–right symmetry [4, 5], R–parity violating SUSY [6–10] and leptoquarks [11, 12]. Finally we discuss the prospects to discriminate different mechanisms.

2 Black Box Theorem

The observation of neutrinoless double beta decay demonstrates that lepton number is violated. Lepton number violation implies that neutrinos have to be Majorana particles. That the two are inseparably connected can be proven by what is known as the black box theorem [2, 3, 13]. Graphically the theorem can be depicted as shown in Fig. 1 (left): If double beta decay has been seen, a Majorana neutrino mass term is generated at higher loop order, even if the underlying particle physics model does not contain a tree-level neutrino mass.

One might wonder, if it is possible to circumvent the connection between Majorana neutrino mass and double beta decay by tuning, for example, in a given model the tree-level and 1-loop contributions to the neutrino mass in such a way that the resulting *observable* neutrino mass is too small to be detected and this is of course possible. However, a tuning order-by-order in perturbation theory requires a stabilizing symmetry for it to be natural

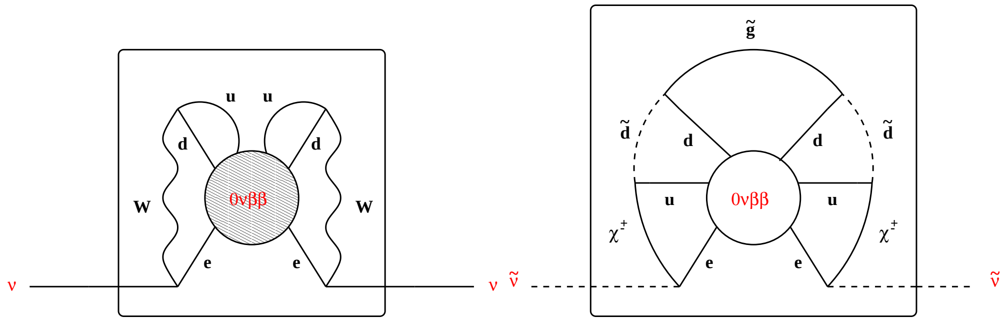

Figure 1: Black box theorem graphically. To the left the original non-supersymmetric "butterfly" diagram, to the right the supersymmetric theorem.

and the black box theorem [2] states that no such symmetry can exist, as has been shown formally in [13].

A word of caution. The black box theorem has often been mis-presented in the literature. It does not guarantee by any means that the mass mechanism of neutrinoless double beta decay is dominant. This can be seen already by looking at the "butterfly" diagram in Fig. 1 (left): If this diagram is the only contribution to the neutrino mass the resulting m_ν is nearly infinitesimal, due to the 4-loop suppression factor. A recent calculation of the diagram in [14] quotes a neutrino mass of the order of $m_\nu \sim 10^{-24}$ eV from current double beta decay limits. However, this does not imply that the neutrino mass has always to be this tiny in order for non-mass-mechanism contributions to double beta decay to dominate. In fact it is easy to find examples for both kinds of particles physics models, those that do give mass mechanism dominance and those that do not. The classic example of the former is the seesaw mechanism, which leaves (in a non-supersymmetric world) double beta decay dominated by neutrino mass *as the only experimental signature*. In the opposite class falls supersymmetry with (trilinear) R–parity violation, see below.

One can also prove a supersymmetric version of the black box theorem [15–17]. This is depicted graphically in Fig. 1 (right). In a supersymmetric theory the scalar partner of the ordinary neutrino is a complex field. Once lepton number is violated, this complex field splits into its real and imaginary components with a non-zero mass difference $\tilde{m}_M^2$. This mass splitting generates lepton number violating effects such as sneutrino to anti-sneutrino oscillations [18,19]. In analogy with the ordinary black box theorem one can show that such a LNV mass splitting in the sneutrino sector leads to double beta decay and observation of double beta decay implies that $\tilde{m}_M^2$ is different from zero. At the same time, Majorana neutrino masses and $\tilde{m}_M^2$ are also always connected and, as shown in [15–17], the existence of one implies the existence of the other (if SUSY indeed is realized).

Finally, we mention that the original version of the black box theorem [2, 3, 13] considers only the first generation of leptons. Oscillation experiments have shown, however, that flavour violation exists in the neutrino sector. It is then possible to prove an extended black box theorem [20], which takes also into account flavour. In essence, this theorem states that under the assumption that all three light neutrinos are Majorana particles, current oscillation data requires the $0\nu\beta\beta$ decay observable m_{ee}, see eq. (1) below, must be different from zero, since no symmetry can exist which guarantees this entry in the neutrino mass matrix to vanish exactly. While academically amusing, however, the theorem can not predict the actual value of m_{ee}, exactly as the original version can not guarantee the dominance of the mass mechanism. Thus, the results of [20] do not guarantee that the double beta decay amplitude is observably large.

3 Lorentz-invariant Description of Neutrinoless Double Beta Decay

We continue by considering the neutrinoless double beta decay rate in a general framework, parametrizing the new physics contributions in terms of all effective low-energy currents allowed by Lorentz-invariance. This parametrization has been developed in [21, 22]. Such an ansatz allows one to separate the nuclear physics part of double beta decay from the underlying particle physics model, and derive limits on arbitrary lepton number violating theories[1].

Before discussing the general decay rate, let us recall that the mass mechanism of double beta decay, measures (or limits) the *effective* Majorana neutrino mass defined as:

$$\langle m_\nu \rangle = \sum_j U_{ej}^2 m_j \equiv m_{ee}. \tag{1}$$

Here, the sum runs over all light neutrinos j with couplings to the electron and a SM W-boson. It is straightforward to show that this quantity is equal to the (ee) entry of the Majorana neutrino mass matrix in the basis where the charged lepton mass matrix is diagonal. For this reason $\langle m_\nu \rangle$ is often also denoted as m_{ee}. This contribution to neutrinoless double beta decay is discussed at length in the contribution by Rodejohann [1] to this issue.

While the general decay rate is independent of the underlying nuclear physics model, to extract quantitative limits values for nuclear matrix elements are needed. Limits discussed below are derived using matrix elements calculated in proton-neutron (pn) QRPA.

[1]For another approach based on an effective operator description compare [23].

For the isotope ^{76}Ge this matrix elements were already available in the literature [7,21,22]. For other isotopes, quoted in the tables below, the numerical values are taken from [24].

Uncertainties in nuclear matrix elements are notoriously difficult to estimate and all limits derived from double beta decay suffer from these uncertainties. Unfortunately, despite all the efforts devoted to the improvement of the matrix element calculations, the latest QRPA matrix elements from the Tübingen group [25] differ from the shell model results revisited, for example, in [26] in many cases by factors of $\sim (2-3)$ in case of the mass mechanism[2]. Moreover, shell model matrix elements are up to now available only for the mass mechanism. Thus uncertainties in other matrix elements, needed in the general decay rate, are even harder to estimate. However, for the long-range part of the amplitude, discussed in section (3.1) we believe that all matrix elements suffer from uncertainties of the same order as those found for the mass mechanism.

For the short-range part of the amplitude, see section (3.2), no other general calculation than the one presented in [22] exists. However, [25] contains matrix elements for heavy neutrino exchange and for the short-range R_P-violating SUSY mechanism, which we can compare to [22]. One noticeable difference is that in [28, 29] it was argued that the effect of short range correlations had been overestimated in earlier calculations. A recalculation of the nuclear matrix elements in [30], using the method proposed in [28], indeed led to an increase of (25-40) % in the numerical values of the nuclear matrix elements. The latest calculation [25] also has short range matrix elements which are larger than those in [22] by similar factors. Despite these more recent calculations we will stick to the matrix elements presented in [7, 21, 22, 24], since (a) no other complete calculation of matrix elements exist and (b) newer matrix elements in existing cases tend to be larger than those of the above publications, i.e. we believe that our limits are conservative.

Currently the most stringent bounds on neutrinoless double beta decay come from ^{76}Ge [31] and ^{136}Xe [32]. Starting from around 2001 [33–35] a small part of the Heidelberg-Moscow collaboration claimed to have observed evidence for neutrinoless double beta decay, but this has so far not been confirmed in any other experiment. In fact, the recent publication of the limit from ^{136}Xe [32] puts some pressure on the claim, although, due to the uncertainty in the nuclear matrix element calculation, ^{136}Xe can not unequivocally rule it out yet. For definiteness we will use the limit from ^{76}Ge of $T_{1/2} \geq 1.9 \times 10^{25}$ ys [31] and the recent result $T_{1/2} \geq 1.6 \times 10^{25}$ ys for ^{136}Xe [32] for the derivation of limits. Results for these two isotopes lead currently to very similar limits, see below[3].

[2]The calculation for ^{136}Xe is a notable exception. Here, the latest shell model matrix element for the mass mechanism [26] agree with [27] within the error bars estimated for the QRPA calculation.

[3]For the mass mechanism, using the nuclear matrix elements from [36], the ^{76}Ge limit corresponds to

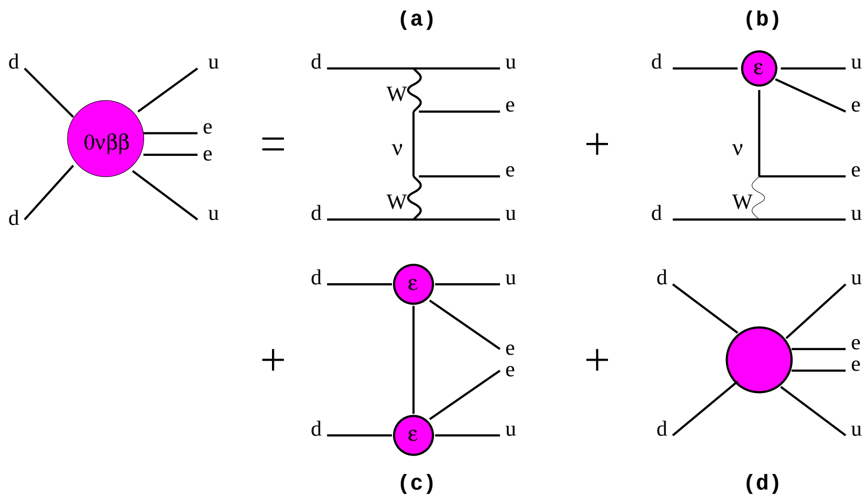

Figure 2: Different contributions to the general double beta rate: The contributions (a) - (c) correspond to the long range part, the contribution (d) is the short range part (from [21]). (a) corresponds to the mass mechanism.

3.1 Long–Range Part

This subsection is essentially based on reference [21]. We consider first the long–range part of neutrinoless double beta decay with two vertices, which are pointlike at the Fermi scale, and exchange of a light neutrino in between. The general Lagrangian can be written in terms of effective couplings $\epsilon^{\alpha}_{\beta}$, which correspond to the pointlike vertices at the Fermi scale so that Fierz rearrangement is applicable,

$$\mathcal{L} = \frac{G_F}{\sqrt{2}} \{ j^{\mu}_{V-A} J^{\dagger}_{V-A,\mu} + {\sum_{\alpha,\beta}}' \epsilon^{\beta}_{\alpha} j_{\beta} J^{\dagger}_{\alpha} \}, \tag{2}$$

with the combinations of hadronic and leptonic Lorentz currents $J^{\dagger}_{\alpha} = \bar{u}\mathcal{O}_{\alpha} d$ and $j_{\beta} = \bar{e}\mathcal{O}_{\beta}\nu$ of defined helicity, respectively. The operators $\mathcal{O}_{\alpha,\beta}$ are defined as

$$\begin{aligned} \mathcal{O}_{V-A} &= \gamma^{\mu}(1-\gamma_5), & \mathcal{O}_{V+A} &= \gamma^{\mu}(1+\gamma_5), \\ \mathcal{O}_{S-P} &= (1-\gamma_5), & \mathcal{O}_{S+P} &= (1+\gamma_5), \\ \mathcal{O}_{T_L} &= \frac{i}{2}[\gamma_{\mu},\gamma_{\nu}](1-\gamma_5), & \mathcal{O}_{T_R} &= \frac{i}{2}[\gamma_{\mu},\gamma_{\nu}](1+\gamma_5). \end{aligned} \tag{3}$$

The prime indicates the sum runs over all contractions allowed by Lorentz–invariance, except for $\alpha = \beta = (V-A)$. Note that all currents have been scaled relative to the strength of the ordinary $(V-A)$ interaction.

$\langle m_\nu \rangle \lesssim 0.35$ eV, while the ^{136}Xe gives $\langle m_\nu \rangle \lesssim 0.34$ eV.

The effective Lagrangian given in eq. (2) represents the most general low-energy 4-fermion charged-current interaction allowed by Lorentz invariance. The interpretation of the effective couplings ϵ_β^α, however, depend on the specific particle physics model. Nevertheless one realizes the following general feature. Using only the SM fermion fields and working in the Majorana basis for the neutrinos ($\nu := \nu_L + \nu_L^C$) it is easily seen that all currents involving operators proportional to $(1+\gamma_5)$ violate lepton number by two units, i.e. the corresponding ϵ_β^α must also be lepton-number violating. Such LNV ϵ_β^α are easily found, an example is given by R–parity violating supersymmetry treated in ref. [7, 10, 37] and discussed later.

The double beta decay amplitude is proportional to the time-ordered product of two effective Lagrangians (see Fig. 2):

$$T(\mathcal{L}_{(1)}\mathcal{L}_{(2)}) = \frac{G_F^2}{2} T\{j_{V-A}J^\dagger_{V-A}j_{V-A}J^\dagger_{V-A} + \epsilon_\alpha^\beta j_\beta J_\alpha^\dagger j_{V-A}J^\dagger_{V-A} + \epsilon_\alpha^\beta \epsilon_\gamma^\delta j_\beta J_\alpha^\dagger j_\delta J_\gamma^\dagger\}. \quad (4)$$

The first term (Fig. 2 (a)) corresponds to the contribution from the Majorana neutrino mass, and the 3rd term (Fig. 2 (c)), which is quadratic in ϵ can be neglected. Only the 2nd term (Fig. 2 (b)) is phenomenologically interesting. For this term one has to consider two general cases:

1) The leptonic SM $(V-A)$ current meets a left–handed non SM current j_β with $\beta = (S-P), T_L$. For this contribution the neutrino propagator is

$$P_L \frac{q^\mu \gamma_\mu + m_\nu}{q_\mu q^\mu - m_\nu^2} P_L = \frac{m_\nu}{q_\mu q^\mu - m_\nu^2}, \quad (5)$$

with the usual left– and right–handed projectors $P_{L/R} = \frac{1\mp\gamma_5}{2}$. This expression is proportional to the unknown Majorana neutrino mass $m_\nu \lesssim 0.5$ eV, for which no lower bound exists. Therefore no limits on the corresponding parameters ϵ_α^β can be derived.

2) The leptonic SM $(V-A)$ current meets a right–handed non SM current j_β with $\beta = (S+P), (V+A), T_R$. For this contribution the neutrino propagator is

$$P_L \frac{q^\mu \gamma_\mu + m_\nu}{q_\mu q^\mu - m_\nu^2} P_R = \frac{q^\mu \gamma_\mu}{q_\mu q^\mu - m_\nu^2}, \quad (6)$$

which is proportional to the neutrino momentum. Since typically $q_\mu \simeq p_F \simeq 100$ MeV with the nuclear Fermi momentum p_F, this part of the amplitude will produce stringent limits on corresponding ϵ_α^β.

Considering only one ϵ_α^β at a time (evaluation "on axis") one can now derive constraints on the effective coupling parameters from a double beta decay half life measurement or bound,

$$[T_{1/2}^{0\nu\beta\beta}]^{-1} = |\epsilon_\alpha^\beta|^2 G_{0k} |ME|^2, \quad (7)$$

where G_{0k} denotes the phase space factors given in [4] and $|ME|$ the nuclear matrix elements discussed below. Note that evaluating "on axis", compared to the arbitrary evaluation, neglects interference terms of the different contributions. Numerical values of the matrix elements $\mathcal{M}_{T'}$, $\mathcal{M}_{GT'}$, $\mathcal{M}_{T''}$, $\mathcal{M}_{GT''}$, $\mathcal{M}_{F'}$ below, calculated in the Quasi Particle Random Phase Approximation (pn-QRPA), are given in Table 2. The matrix elements for the different contributions are defined as follows.

SM meets $j_{V+A}J^\dagger_{V+A}$ and $j_{V+A}J^\dagger_{V-A}$ These combinations of currents and the corresponding matrix elements have been discussed in the literature before [4, 5, 36]. Matrix elements have been calculated in different papers, and we will follow [5].

SM meets $j_{S+P}J^\dagger_{S+P}$ and $j_{S+P}J^\dagger_{S-P}$ Using s-wave approximation for the outgoing electrons and some assumptions according to [9, 38] one has

$$ME^{S+P}_{S+P} = -ME^{S+P}_{S-P} = -\frac{F_P^{(3)}(0)}{Rm_e G_A}\Big(\mathcal{M}_{T'} + \frac{1}{3}\mathcal{M}_{GT'}\Big), \tag{8}$$

with the phase space factor G_{01} and the Gamov-Teller and tensor matrix elements $\mathcal{M}_{GT'}$ and $\mathcal{M}_{T'}$, respectively. In addition, R denotes the nuclear radius, m_e the electron mass, $G_A \simeq 1.26$ and $F_P^{(3)}(0) = 4.41$ [39].

SM meets $j_{T_R}J^\dagger_{T_R}$ and $j_{T_R}J^\dagger_{T_L}$ The hadronic T_R contribution is given by

$$ME^{T_R}_{T_R} = -\alpha_1\frac{2}{3}\mathcal{M}_{GT'} + \alpha_1\mathcal{M}_{T'}, \tag{9}$$

with an effective nuclear form factor α_1. For the hadronic T_L contribution in leading order of the inverse proton mass ($1/m_p$) one finds

$$ME^{T_R}_{T_L} = \alpha_2\mathcal{M}_{F'} - \alpha_3\Big(\mathcal{M}_{T''} + \frac{1}{3}\mathcal{M}_{GT''}\Big), \tag{10}$$

with nuclear matrix elements $\mathcal{M}_{F'}$, $\mathcal{M}_{GT''}$ and $\mathcal{M}_{T''}$ and effective nuclear form factors α_2 and α_3. The parameters α_i are defined as:

$$\alpha_1 = \frac{4T_1^{(3)}(0)G_V(1-2m_p(G_W/G_V))}{G_A^2 Rm_e}, \tag{11}$$

$$\alpha_2 = \frac{4(2\hat{T}_2^{(3)}(0) - T_1^{(3)}(0))G_V}{G_A^2 Rm_e}, \tag{12}$$

$$\alpha_3 = \frac{4T_1^{(3)}(0)(G_P/G_A)}{G_A R^2 m_e}. \tag{13}$$

Isotope	G_{01}	G_{06}	G_{09}
^{76}Ge	$6.40 \cdot 10^{-15}$	$1.43 \cdot 10^{-12}$	$3.30 \cdot 10^{-10}$
^{82}Se	$2.82 \cdot 10^{-14}$	$4.77 \cdot 10^{-12}$	$1.32 \cdot 10^{-9}$
^{100}Mo	$4.58 \cdot 10^{-14}$	$7.09 \cdot 10^{-12}$	$1.88 \cdot 10^{-9}$
^{128}Te	$1.83 \cdot 10^{-15}$	$4.94 \cdot 10^{-13}$	$7.52 \cdot 10^{-11}$
^{130}Te	$4.44 \cdot 10^{-14}$	$6.89 \cdot 10^{-12}$	$1.55 \cdot 10^{-9}$
^{136}Xe	$4.73 \cdot 10^{-14}$	$7.28 \cdot 10^{-12}$	$1.60 \cdot 10^{-9}$
^{150}Nd	$2.10 \cdot 10^{-13}$	$2.48 \cdot 10^{-11}$	$6.45 \cdot 10^{-9}$

Table 1: Phase space factors for the general decay rate, numerical values taken from the calculation of [4].

Here, $T_1^{(3)} = 1.38$, $\hat{T}_2^{(3)} = -4.54$ [39], $G_P/G_A = 2m_p/m_\pi^2$ and $(G_W/G_V) = \frac{\mu_p - \mu_n}{2m_p} \simeq \frac{-3.7}{2m_p}$ is obtained from the CVC hypothesis. Numerical values for the matrix elements and limits on the ϵ_β^α are discussed in Section 3.3.

3.2 Short–Range Part

In the short range part the effective interaction can be considered as point-like, thus the decay rate results from the following general Lorentz invariant Lagrangian[4]:

$$\mathcal{L} = \frac{G_F^2}{2} m_p^{-1} \{\epsilon_1 JJj + \epsilon_2 J^{\mu\nu} J_{\mu\nu} j + \epsilon_3 J^\mu J_\mu j + \epsilon_4 J^\mu J_{\mu\nu} j^\nu + \epsilon_5 J^\mu J j_\mu\}, \tag{14}$$

with the hadronic currents of defined chirality $J = \overline{u}(1 \pm \gamma_5)d$, $J^\mu = \overline{u}\gamma^\mu(1 \pm \gamma_5)d$, $J^{\mu\nu} = \overline{u}\frac{i}{2}[\gamma^\mu, \gamma^\nu](1 \pm \gamma_5)d$ and the leptonic currents $j = \overline{e}(1 \pm \gamma_5)e^C$, $j^\mu = \overline{e}\gamma^\mu(1 \pm \gamma_5)e^C$. In some of the cases the decay rate for the effective coupling ϵ_α depends also on the chirality of the currents involved. In these cases we define $\epsilon_\alpha = \epsilon_\alpha^{xyz}$, where $xyz = L/R, L/R, L/R$ defines the chirality of the hadronic and leptonic currents in the order of appearance in eq. (14). In the cases where it is not necessary to distinguish the different chiralities we suppress this additional index.

In renormalizable theories no fundamental tensors exist. Thus the tensor currents have to result either from Fierz rearrangements or by integrating out heavy particles, when deriving the effective Lagrangian from the fundamental theory and decomposing the expressions obtained in terms of the Lorentz invariant bilinears used above, e.g. from $\bar{u}\gamma_\mu\gamma_\nu(1+\gamma_5)d = g_{\mu\nu}J - iJ_{\mu\nu}$. Applying the standard nuclear theory methods based on the non-relativistic impulse approximation one derives the general $0\nu\beta\beta$-decay half-life formula

[4]Here we follow the essentially the calculations presented in [22], see however, Table 2.

Isotope	$\mathcal{M}_{GT'}$	$\mathcal{M}_{F'}$	$\mathcal{M}_{GT''}$	$\mathcal{M}_{T'}$	$\mathcal{M}_{T''}$	$\mathcal{M}_{GT,N}$	$\mathcal{M}_{F,N}$
^{76}Ge	2.95	-0.663	8.78	0.224	1.33	0.113	-0.0407
^{82}Se	2.71	-0.603	7.96	0.208	1.26	0.102	-0.0360
^{100}Mo	3.69	-0.876	13.4	0.328	2.44	0.129	-0.0489
^{116}Cd	2.26	-0.509	7.13	0.193	1.47	0.075	-0.0271
^{128}Te	3.70	-0.814	13.4	0.331	2.37	0.119	-0.0419
^{130}Te	3.27	-0.720	12.0	0.304	2.20	0.105	-0.0369
^{136}Xe	1.83	-0.403	6.90	0.165	1.18	0.058	-0.0203
^{150}Nd	5.39	-1.21	21.8	0.642	5.07	0.165	-0.0591

Table 2: Nuclear matrix elements for $0\nu\beta\beta$ decay calculated in the pn-QRPA approach. Results of different publications [7, 21, 22, 24] are summarized here. Note that the isotope ^{150}Nd has a sizeable deformation, but the calculation is performed in the spherical limit. The numbers for ^{150}Nd might therefore be an overestimation of the true values.

in s–wave approximation

$$[T_{1/2}^{0\nu\beta\beta}]^{-1} = G_1 \left| \sum_{i=1}^{3} \epsilon_i \mathcal{M}_i \right|^2 + G_2 \left| \sum_{i=4}^{5} \epsilon_i \mathcal{M}_i \right|^2 + G_3 \mathrm{Re} \left[\left(\sum_{i=1}^{3} \epsilon_i \mathcal{M}_i \right) \left(\sum_{i=4}^{5} \epsilon_i \mathcal{M}_i \right)^* \right]. \quad (15)$$

Here the phase space factors are

$$G_1 = G_{01}, \quad G_2 = \frac{(m_e R)^2}{8} G_{09}, \quad G_3 = \left(\frac{m_e R}{4} \right) G_{06}, \quad (16)$$

with G_{0k} calculated in [4] and shown in Table 1 for completeness. The nuclear matrix elements in eq. (15) are defined as[5]

$$\begin{aligned} \mathcal{M}_1 &= -\alpha_1^{SR} \mathcal{M}_{F,N}, \quad \mathcal{M}_2 = -\alpha_2^{SR} \mathcal{M}_{GT,N}, \\ \mathcal{M}_3 &= \frac{m_A^2}{m_p m_e} \{ \mathcal{M}_{GT,N} \mp \alpha_3^{SR} \mathcal{M}_{F,N} \}, \\ \mathcal{M}_4 &= \pm \alpha_4^{SR} \mathcal{M}_{GT,N}, \quad \mathcal{M}_5 = \mp \alpha_5^{SR} \mathcal{M}_{F,N}. \end{aligned} \quad (17)$$

In the last three cases contractions of hadronic currents with different chiralities lead to different results. The negative sign in $\mathcal{M}_3$ corresponds to ϵ_3^{LLz} and ϵ_3^{RRz} ($J_{V\mp A} J_{V\mp A}$), the positive sign to ϵ_3^{LRz} and ϵ_3^{RLz} ($J_{V\mp A} J_{V\pm A}$). The sign of $\mathcal{M}_4$ is positive for the combinations ϵ_4^{LLL}, ϵ_4^{RRL}, ϵ_4^{RLR}, ϵ_4^{LRR} ($J_{V\mp A} J_{TL/TR} j_{V-A}$ and $J_{V\pm A} J_{TL/TR} j_{V+A}$). For the combinations ϵ_4^{LLR}, ϵ_4^{RRR}, ϵ_4^{RLL}, ϵ_4^{LRL} ($J_{V\mp A} J_{TL/TR} j_{V+A}$ and $J_{V\pm A} J_{TL/TR} j_{V-A}$) it is negative. The sign of the matrix element $\mathcal{M}_5$ is negative for the left-handed leptonic current (ϵ_5^{xyL}) and positive

[5] Note that the α_i in the long-range part and the α_i^{SR} defined here are different coefficients.

Isotope	$\lvert\epsilon_{V-A}^{V+A}\rvert$	$\lvert\epsilon_{V+A}^{V+A}\rvert$	$\lvert\epsilon_{S-P}^{S+P}\rvert$	$\lvert\epsilon_{S+P}^{S+P}\rvert$	$\lvert\epsilon_{TL}^{TR}\rvert$	$\lvert\epsilon_{TR}^{TR}\rvert$
^{76}Ge	$3.5 \cdot 10^{-9}$	$6.2 \cdot 10^{-7}$	$1.1 \cdot 10^{-8}$	$1.1 \cdot 10^{-8}$	$6.7 \cdot 10^{-10}$	$1.1 \cdot 10^{-9}$
^{136}Xe	$2.8 \cdot 10^{-9}$	$5.6 \cdot 10^{-7}$	$6.8 \cdot 10^{-9}$	$6.8 \cdot 10^{-9}$	$4.8 \cdot 10^{-10}$	$8.1 \cdot 10^{-10}$

Table 3: Limits on effective long-range $B-L$ violating couplings. These limits are derived assuming only one ϵ is different from zero at a time. With the recent limit on the half-live for ^{136}Xe [32], ^{136}Xe now gives limits competitive with or better than ^{76}Ge.

for the right-handed one (ϵ_5^{xyR}). The numerical values of the standard nuclear matrix elements $\mathcal{M}_{F,N}$ and $\mathcal{M}_{GT,N}$ in eq. (17), calculated in the Quasi Particle Random Phase Approximation (pn-QRPA), are given in Table 2. The pre-factors α_i^{SR} in eq. (17) are defined as follows,

$$\alpha_1^{SR} = \left(\frac{F_S^{(3)}}{G_A}\right)^2 \frac{m_A^2}{m_p m_e}, \quad \alpha_2^{SR} = 8\left(\frac{T_1^{(3)}}{G_A}\right)^2 \frac{m_A^2}{m_p m_e},$$
$$\alpha_3^{SR} = \left(\frac{g_V}{G_A}\right)^2, \quad \alpha_4^{SR} = \frac{T_1^{(3)}}{G_A}\frac{m_A^2}{m_p m_e}, \quad \alpha_5^{SR} = \frac{g_V F_S^{(3)}}{G_A^2}\frac{m_A^2}{m_p m_e}. \tag{18}$$

The finite nucleon size is taken into account in a common way [40, 41] by introducing the nucleon form factors in a dipole form

$$\frac{g_{V,A}(q^2)}{g_{V,A}} = \frac{F_S(q^2)}{F_S} = \frac{T_1^{(3)}(q^2)}{T_1^{(3)}} = \left(1 - \frac{q^2}{m_A^2}\right)^{-2}, \tag{19}$$

with $m_A = 0.85$ GeV, $g_V = 1.0, G_A = 1.26$. The other form factor normalizations have been calculated in ref. [39] within the MIT bag model, $F_S^{(3)} = 0.48$.

3.3 General $0\nu\beta\beta$ Constraints

We list all nuclear matrix elements necessary for deriving limits for the eight most important nuclear isotopes in Table 2. The long range NMEs for ^{76}Ge had been published previously in [21]. The long-range matrix elements for other isotopes are from [24]. Note that the numerical values for ^{150}Nd might overestimate the true NMEs, since the calculation was done in the spherical limit. With these matrix elements we find the limits on the different contributions presented in Tables 3 and 4.

A few comments on tables (3) and (4) might be in order. The $j_{V+A}J^\dagger_{V+A}$ and $j_{V+A}J^\dagger_{V-A}$ part of the amplitude has been considered within left-right symmetric models [4, 5, 36]. In our notation, the limits are given as ϵ_{V+A}^{V+A} and ϵ_{V-A}^{V+A}. In the notation of [4] these correspond to $\langle\lambda\rangle = \epsilon_{V+A}^{V+A}$ and $\langle\eta\rangle = \epsilon_{V-A}^{V+A}$. Note also, that we have updated the

^{A}X	$\|\epsilon_1\|$	$\|\epsilon_2\|$	$\|\epsilon_3^{LLz(RRz)}\|$	$\|\epsilon_3^{LRz(RLz)}\|$	$\|\epsilon_4\|$	$\|\epsilon_5\|$
^{76}Ge	$3.2 \cdot 10^{-7}$	$1.8 \cdot 10^{-9}$	$2.2 \cdot 10^{-8}$	$1.4 \cdot 10^{-8}$	$1.5 \cdot 10^{-8}$	$1.5 \cdot 10^{-7}$
^{136}Xe	$2.6 \cdot 10^{-7}$	$1.4 \cdot 10^{-9}$	$1.1 \cdot 10^{-8}$	$1.7 \cdot 10^{-8}$	$1.2 \cdot 10^{-8}$	$1.2 \cdot 10^{-7}$

Table 4: Limits on effective short-range $B-L$ violating couplings. These limits are derived assuming only one ϵ is different from zero at a time. For ϵ_3 the contractions of hadronic currents with different chiralities lead to different results. With the recent limit on the half-live for ^{136}Xe [32], ^{136}Xe now gives limits competitive with or better than ^{76}Ge.

limits with the half-live limits from [31] for ^{76}Ge and for ^{136}Xe from [32]. All limits are derived "on axis", i.e. assuming only one non-zero contribution at a time.

4 Models of Lepton Number Violation

In the following we discuss several prominent new physics models that incorporate lepton number violation and which lead to potentially observable rates for neutrinoless double beta decay. The list of models presented here is not intended to be exhaustive, as there is a large number of alternative schemes which produce interesting $0\nu\beta\beta$ phenomenology such as scalar bilinears [42] or a scalar octet seesaw mechanism [43, 44]. A large range of models is discussed in the review [45] and in the references therein.

4.1 Left-Right Symmetry

As a first example of a model incorporating a rich phenomenology of lepton number violation, we will discuss the minimal Left-Right symmetric model (LRSM) which extends the Standard Model gauge symmetry to the group $\mathrm{SU}(2)_L \otimes \mathrm{SU}(2)_R \otimes \mathrm{U}(1)_{B-L}$ [46–49]. Right-handed neutrinos are a necessary ingredient to realize this extended symmetry and are part of an $\mathrm{SU}(2)_R$ doublet. In the LRSM, a generation of leptons is assigned to the multiplets $L_i = (\nu_i, l_i)$ with the quantum numbers $Q_{L_L} = (1/2, 0, -1)$ and $Q_{L_R} = (0, 1/2, -1)$ under $\mathrm{SU}(2)_L \otimes \mathrm{SU}(2)_R \otimes \mathrm{U}(1)_{B-L}$. The Higgs sector contains a bidoublet ϕ and two triplets Δ_L and Δ_R. The VEV v_R of Δ_R breaks $\mathrm{SU}(2)_R \otimes \mathrm{U}(1)_{B-L}$ to $\mathrm{U}(1)_Y$ and generates masses for the right-handed W_R and Z_R gauge bosons, and the heavy neutrinos. Since right-handed currents and particles have not been observed, v_R has to be sufficiently large. The neutral part of the bidoublet acquires a VEV v at the electroweak scale thereby breaking the SM symmetry. The LRSM can accommodate a general 6×6 neutrino mass matrix in the basis

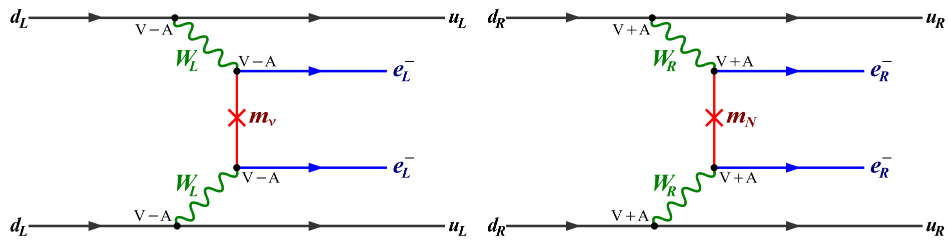

Figure 3: $0\nu\beta\beta$ in the LRSM: Light (left) and heavy (right) neutrino exchange.

$(\nu_L, \nu_L^c)^T$,

$$\mathcal{M} = \begin{pmatrix} M_L & M_D \\ M_D^T & M_R \end{pmatrix}, \tag{20}$$

with Majorana and Dirac mass entries of the order $M_L \approx y_M v_L$, $M_R \approx y_M v_R$ and $M_D = y_D v$. Here $y_{M,D}$ are Yukawa couplings and v_L is the VEV of the left Higgs triplet, which together with the other vacuum expectation values satisfies $v_L v_R = v^2$. The mass matrix (20) is diagonalized by a mixing matrix of the form

$$\mathcal{U} = \begin{pmatrix} U & W \\ W^T & V \end{pmatrix}, \tag{21}$$

with the 3×3 block matrices U and V describing the mixing among the light and heavy neutrinos, respectively, whereas W yields left-right mixing between the light and heavy states.

4.1.1 Neutrinoless Double Beta Decay

In the LRSM, several mechanisms can contribute to $0\nu\beta\beta$ as shown in Figs. 3, 4 and 5. The contributions in Figs. 3 and 4 are of the same diagramatical form with the exchange of either light or heavy neutrinos as well as light and heavy W bosons. Diagram 3 (left) describes the standard mechanism of light neutrino exchange, with the effective mass $m_{ee} = |\sum_i U_{ei}^2 m_{\nu_i}|$, saturating current experimental bounds if the light neutrinos are degenerate at a mass scale $m_{\nu_1} \approx m_{ee} \approx 0.3 - 0.6$ eV. Correspondingly, diagram 3 (right) describes the exchange of heavy right-handed neutrinos. In the classification of Section 3, this is a realization of the short-range operator with the effective coupling ϵ_3^{RRz}. Assuming manifest left-right symmetry, i.e. $g_R \equiv g_R$, in terms of the LRSM model parameters it is given by

$$\epsilon_3^{RRz} = \sum_{i=1}^{3} V_{ei}^2 \frac{m_p}{m_{N_i}} \frac{m_{W_L}^4}{m_{W_R}^4}, \tag{22}$$

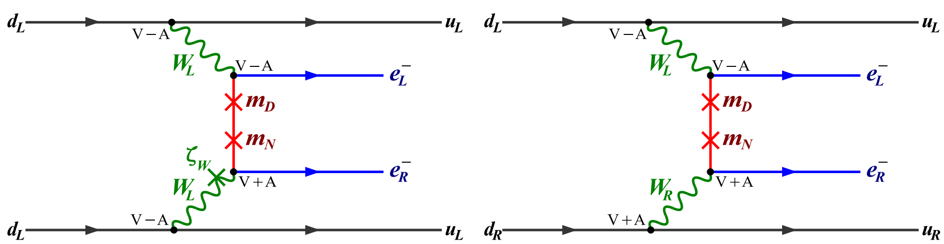

Figure 4: $0\nu\beta\beta$ in the LRSM: Light neutrino exchange not proportional to the neutrino mass, with a left-handed (left) and right-handed (right) hadronic current.

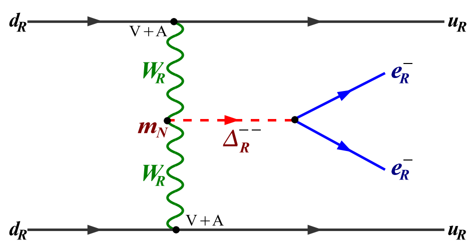

Figure 5: $0\nu\beta\beta$ in the LRSM: Doubly-charged Higgs Triplet exchange.

and searches for $0\nu\beta\beta$ yield the limit $|\epsilon_3^{RRz}| < 1.1 \cdot 10^{-8}$ (cf. Table 4).

Because of the presence of right-handed currents in the LRSM, light neutrino exchange does not necessarily require a chirality violating mass insertion. As a consequence, the outgoing electrons can have opposite chirality, and the contributions are suppressed either by the heaviness of W_R or the smallness of the mixing angle ζ of the W bosons as shown in Fig. 4. The coupling parameters of the corresponding effective long-range operators can be written as

$$\epsilon_{V+A}^{V+A} = \sum_{i=1}^{3} U_{ei} W_{ei} \frac{m_{W_L}^2}{m_{W_R}^2}, \qquad \epsilon_{V-A}^{V+A} = \sum_{i=1}^{3} U_{ei} W_{ei} \tan\zeta, \tag{23}$$

with the current experimental limits $|\epsilon_{V+A}^{V+A}| < 5.6 \cdot 10^{-7}$ and $|\epsilon_{V-A}^{V+A}| < 2.8 \cdot 10^{-9}$, respectively (cf. Table 3). Both cases are necessarily suppressed by the left-right neutrino mixing $M_D/M_N \sim \sqrt{m_\nu/m_N}$ (the latter expression is valid for a dominant type-I seesaw mass mechanism [50]) between light and heavy neutrinos.

Finally, Fig. 5 describes the exchange of a right-handed doubly-charged triplet Higgs Δ_R, which has the same effective operator structure as heavy neutrino exchange. The

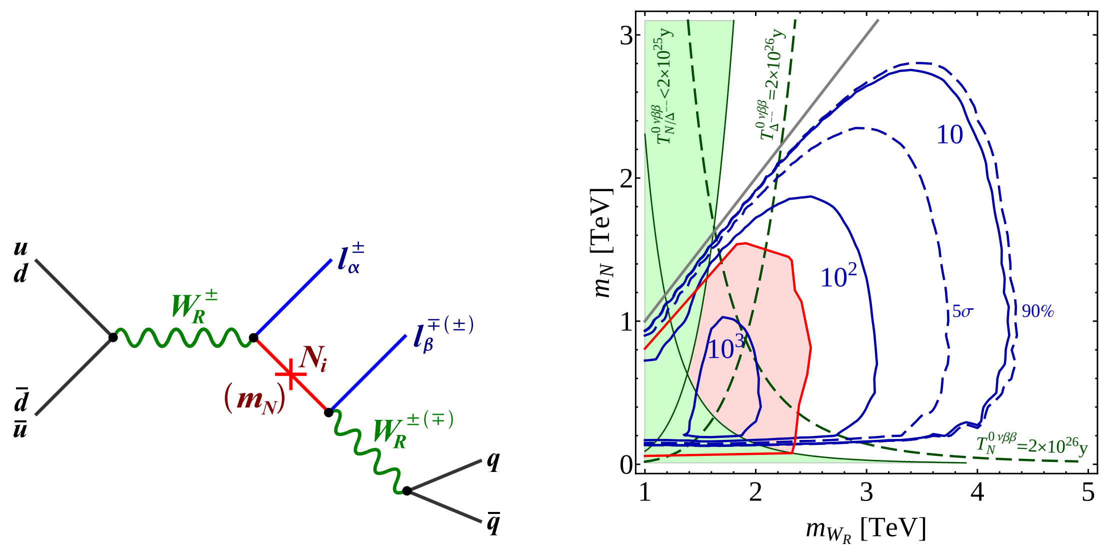

Figure 6: Production and decay of a heavy right-handed neutrino with dilepton signature at hadron colliders (left). Comparison of LNV event rates at the LHC and in $0\nu\beta\beta$ experiments (right, from [51]). The solid blue contours give the number of $e^\pm e^\pm + 2j$ events at the LHC with 14 TeV and $\mathcal{L} = 30$ fb^{-1}. The dashed blue contours correspond to signal significances of 5σ and 90%. The shaded green area denotes the parameter space excluded by $0\nu\beta\beta$ at $T^{0\nu\beta\beta} \approx 2 \times 10^{25}$ years, assuming dominant doubly-charged Higgs or heavy neutrino exchange. The green dashed contours show the sensitivity of future $0\nu\beta\beta$ experiments at $T^{0\nu\beta\beta} \approx 2 \times 10^{26}$ years. The red shaded area is excluded by LHC searches [52].

effective short-range coupling strength is here given as

$$\epsilon_3^{RRz} = \sum_{i=1}^{3} V_{ei}^2 \frac{m_{N_i} m_p}{m_{\Delta_R}^2} \frac{m_{W_L}^4}{m_{W_R}^4}, \tag{24}$$

currently limited to $|\epsilon_3^{RRz}| < 1.1 \times 10^{-8}$ (cf. Table 4). The heavy neutrino masses m_{N_i} appear since in Figure 5 the coupling of the Higgs triplet to the gauge boson is proportional to v_R and the electron vertex is of Yukawa strength $(y_M)_{ee}$.

4.1.2 Lepton Number Violation at the LHC

In [51], the potential to discover number violating dilepton signals $pp \to W_R \to e^\pm \mu^{\pm,\mp} + 2$ jets via a heavy right-handed neutrino at the LHC was determined, cf. Fig. 6 (left). Fig. 6 (right) compares the LHC event rates for such lepton number violation processes with the sensitivity of $0\nu\beta\beta$ experiments. The green regions and green dashed contours represent the excluded areas from $0\nu\beta\beta$ searches using nominal values for the current limit

($T^{0\nu\beta\beta} \gtrsim 2\times10^{25}$ years) and the future sensitivity ($T^{0\nu\beta\beta} \approx 2\times10^{26}$ years). In this analysis it was assumed that left-right mixing is negligible and $0\nu\beta\beta$ is either dominated by heavy neutrino or Higgs triplet exchange. As the contribution from the standard light neutrino exchange is always present, the these results correspond to a scenario with a small effective mass m_{ee}. Fig. 6 (right) gives an example of the possible interplay between searches for lepton number violation at a high energy collider and in $0\nu\beta\beta$ experiments.

4.2 R–Parity Violating Supersymmetry

The MSSM (minimal supersymmetric extension of the standard model) assumes a discrete Z_2 symmetry, called R-=parity (R_P), exists. This symmetry guarantees the lightest supersymmetric particle to be stable, thus the MSSM with R_P offers a dark matter candidate. However, from a theoretical perspective the MSSM does not offer any explanation as to why R_P is conserved. Rather it is an ad hoc symmetry to avoid a phenomenological disaster. Consider the R_P violating terms

$$W_{\not R_p} = \lambda_{ijk}L_iL_j\bar{E}_k + \lambda'_{ijk}L_iQ_j\bar{D}_k + \epsilon_iL_iH_u + \lambda''_{ijk}\bar{U}_i\bar{D}_j\bar{D}_k, \tag{25}$$

where indices i, j, k label generations. The first three terms violate lepton number, while the last one violates baryon number. In the presence of both types of terms the proton decays at a rate which is many orders of magnitude above the experimental bound. However, any discrete symmetry which eliminates either the baryon or the lepton number violating terms is phenomenologically acceptable [53]. In fact, since the lepton number violating terms in eq. (25) generate Majorana neutrino masses, a small amount of R_P violation could actually explain the observed neutrino oscillation data [54].

4.2.1 Neutrinoless Double Beta Decay

In the case that R_P is broken, $0\nu\beta\beta$ decay can occur through Feynman graphs involving the exchange of superpartners as well as $\not R_P$–couplings λ' [6, 7, 9, 10]. The short-range contribution has been discussed in [6, 7]. Here, we take the opportunity to correct some errors in the original publication [7], which leads to a slight change in the numerical values of the published matrix elements: (i) In the coupling constants $\alpha^{(i)}_{A/V}$ of [7], eqs. (57)-(60), one should replace $T_2^{(3)} \to \hat{T}_2^{(3)}$. (ii) In Section V of [7] five different nuclear matrix elements are defined. The tensor matrix element should be written as $\mathcal{M}_{T'} \sim (\sigma_\mathbf{i} \cdot \hat{\mathbf{r}}_\mathbf{ij})(\sigma_\mathbf{j} \cdot \hat{\mathbf{r}}_\mathbf{ij}) - 1/3\sigma_\mathbf{i} \cdot \sigma_\mathbf{j}$. And, finally (iii) there was a numerical error in the code, which converted Table II to Table III in [7]. The corrected values for the nuclear matrix element $\mathcal{M}_{\tilde{q}}$ are given in

^{A}Y	^{76}Ge	^{82}Se	^{100}Mo	^{116}Cd	^{128}Te	^{130}Te	^{136}Xe	^{150}Nd
A) $\mathcal{M}_{\tilde{q}}$	222	199	265	150	242	214	116	353
B) $\mathcal{M}_{\tilde{q}}$	281	251	331	190	301	266	145	432

Table 5: Nuclear matrix elements for short-range SUSY $0\nu\beta\beta$ decay. Shown are $\mathcal{M}_{\tilde{q}}$ for the two sets of input values of coefficients for the $\alpha^{(i)}$ of Table 1 in [7], corrected for the errors discussed in the text.

Table 5. As in the original paper, $-\mathcal{M}_{\tilde{q}}$ is given, to account for a relative sign in the neutrino mass mechanism with respect to the definitions used in the formalism of Doi, Kotani and Takasugi [4]. Note that the R_P violating SUSY mechanism depends on a combination of different short-range matrix elements discussed in section (3.2), since in the amplitude both JJj and $J^{\mu\nu}J_{\mu\nu}j$ currents appear.

Ref. [7] used the half-live limit from the Heidelberg-Moscow collaboration available at that time [55], which was later superseded by the more stringent value of [31]. The change in the matrix element and the update in the half-life combined leads to a slightly more stringent limit on $\lambda^{'}_{111}$ given by

$$\lambda^{'}_{111} \leq 2.6 \cdot 10^{-4}\Big(\frac{m_{\tilde{q}}}{100 \text{ GeV}}\Big)^{2}\Big(\frac{m_{\tilde{g}}}{100 \text{ GeV}}\Big)^{1/2}, \tag{26}$$

for $m_{\tilde{d}_R} = m_{\tilde{u}_L}$. For comparison, from ^{136}Xe data [32] one gets currently $\lambda^{'}_{111} \leq 2.7 \cdot 10^{-4}$. Note, that recently [25] published sets of matrix elements for R_P violating double beta decay for the pion-exchange mechanism, which are, depending on the choice of nucleon-nucleon interaction, model space and value of G_A, between a factor of $x \sim (2-3)$ larger than the matrix elements of Table 5. These would lead to limits on $\lambda^{'}_{111}$ which are stronger by a corresponding factor of $\sqrt{x}$.

$0\nu\beta\beta$ decay is not only sensitive to $\lambda^{'}_{111}$. Taking into account the fact that the SUSY partners of the left- and right–handed quark states can mix with each other, new diagrams appear in which the neutrino-mediated double beta decay is accompanied by SUSY exchange in the vertices [8–10]. A calculation of previously neglected tensor contributions to the decay rate allows to derive improved limits on different combinations of $\lambda^{'}$ [10]. Assuming the supersymmetric mass parameters of order 100 GeV, the half life limit of the Heidelberg–Moscow Experiment implies: $\lambda^{'}_{113}\lambda^{'}_{131} \leq 3 \cdot 10^{-8}$, $\lambda^{'}_{112}\lambda^{'}_{121} \leq 1 \cdot 10^{-6}$.

4.2.2 Lepton Number Violation at the LHC

Similar to the situation in left-right symmetric models, also in R–parity violating SUSY scenarios interesting and complementary information can be obtained from the neutrinoless double beta decay analogue at the LHC, namely resonant single selectron production with two like sign electrons in the final state [56, 57]. The color and spin-averaged parton total cross section of a single slepton production is given by [58]

$$\hat{\sigma} = \frac{\pi}{12\hat{s}} |\lambda'_{111}|^2 \delta \left(1 - \frac{m_{\tilde{l}}^2}{\hat{s}} \right) , \tag{27}$$

where $\hat{s}$ is the partonic center of mass energy, $m_{\tilde{l}}$ is the mass of the resonant slepton, and finite width effects have been neglected. Considering effects from parton distribution functions, to a good approximation the total cross section scales like $\sigma(pp \to \tilde{l}) \propto |\lambda'_{111}|^2/m_{\tilde{l}}^3$ with the slepton mass in the parameter region of interest.

Thus for small slepton masses, the stringent bound from $0\nu\beta\beta$ decay makes this process unobservable at the LHC. However, the bound on λ'_{111} originating from the non-observation of $0\nu\beta\beta$ decay scales with the slepton mass like $\sigma < c\Lambda^2_{SUSY}$ where c is a constant, so that for higher values of the SUSY masses, larger cross-sections may be allowed as much a larger λ'_{111} is no longer excluded. It is this possibility that can be exploited at the LHC.

In [56,57] it has been shown that much of the parameter space allowed by $0\nu\beta\beta$ decay in simple models of supersymmetry breaking actually predicts observable single slepton production at the LHC (compare Fig. 7). Moreover, if the next generation of experiments observe $0\nu\beta\beta$ decay, the LHC has a very good chance of observing single slepton production with only 10 fb^{-1} of integrated luminosity, assuming that $0\nu\beta\beta$ decay is induced by a λ'_{111} coupling. On the other hand, non-observation of single slepton production could then discriminate against the λ'_{111} mechanism. In general, both Majorana neutrino masses and λ'_{111} could contribute simultaneously and non-negligibly to $0\nu\beta\beta$ decay. In this case detailed LHC measurements of the kinematics in single slepton production could constrain the SUSY parameters, and the total cross-section could then give information about the size of $|\lambda'_{111}|$. In principle and depending on nuclear matrix element uncertainties the LHC information could be combined to predict an associated inverse double beta decay half life coming from λ'_{111}, which could be compared with the experimental half life measurement in order to see if additional contributions were necessary.

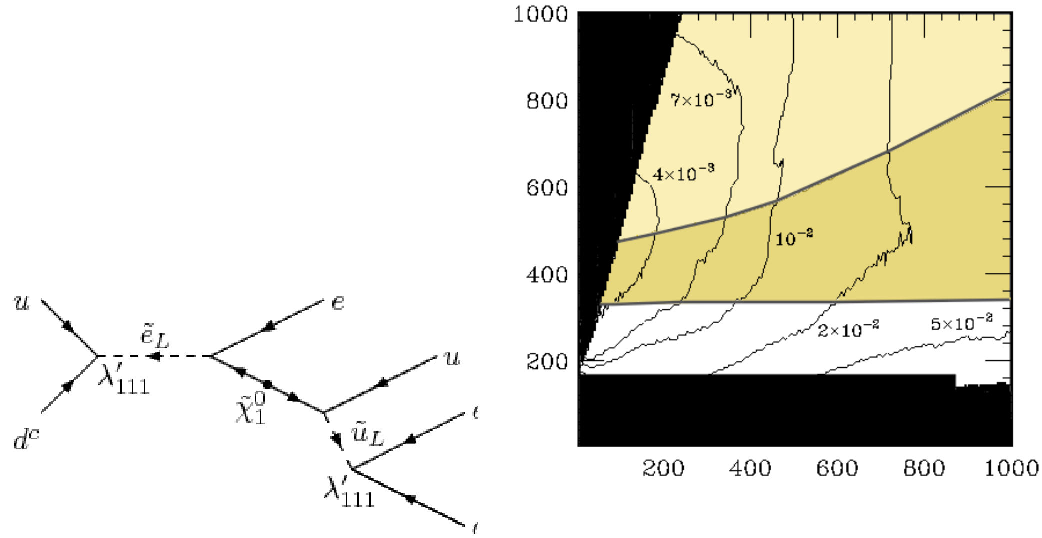

Figure 7: Production and decay of a single selectron in R–parity violating models (left, from [56]) . Region in the mSUGRA parameter space (vertical axis: $M_{1/2}$ in GeV, horizontal axis: M_0 in GeV) in which single slepton production may be observed at the LHC for $\tan\beta = 10$, $A_0 = 0$ and 10fb^{-1} of integrated luminosity. In the top left-hand black triangle, the stau is the LSP, a case not discussed in [56]. The black region at the bottom is ruled out by direct search constraints. The labeled contours are taken from Ref. [59], and indicate the search reach given by the corresponding value of λ'_{111}. The white, dark-shaded and light-shaded regions demonstrate that observation of single slepton production at the 5σ level would imply $T_{1/2}^{0\nu\beta\beta} < 1.9\cdot 10^{25}$yrs, $100 > T_{1/2}^{0\nu\beta\beta}/10^{25}$yrs > 1.9 and $T_{1/2}^{0\nu\beta\beta} > 1\times 10^{27}$yrs, respectively (right, from [56]).

4.3 Leptoquarks

Leptoquarks (LQs) are hypothetical scalar or vector particles coupling to both leptons and quarks. They appear most prominently in grand unified theories, but also in extended Technicolor or Compositeness models. LQs which conserve baryon number can be relatively light [60], possibly within reach of accelerator experiments. Also low-energy precision measurements can give limits on LQ properties, for a detailed list on constraints from non-accelerator searches see, for example [61] and [62]. The mixing of different LQ multiplets by a possible leptoquark–Higgs coupling [11] can lead to a contribution to $0\nu\beta\beta$ decay, if these couplings violate lepton number [12]. Diagrams involving LQs and standard model weak current interactions can be generated, see Fig. 8. These diagrams are of the long range type and due to the chirality violating LQ interaction gain a $\not{p}$ -enhancement in the double

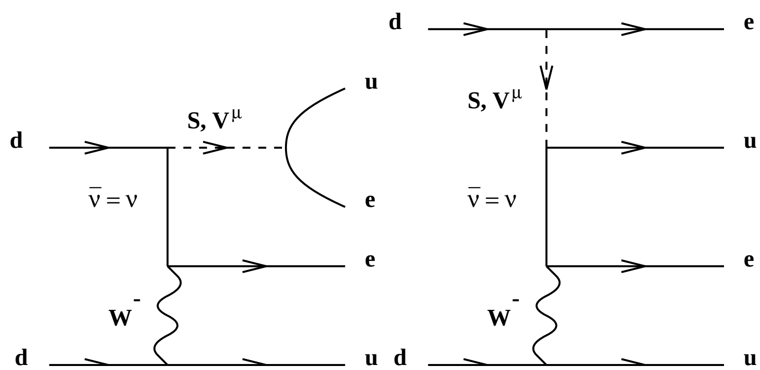

Figure 8: Leptoquark diagrams for neutrinoless double beta decay.

beta decay amplitude. Combined with a lower limit on the $0\nu\beta\beta$ decay half–life bounds on effective couplings can be derived [12]. Assuming only one lepton number violating $\Delta L = 2$ LQ–Higgs coupling unequal to zero and the leptoquark masses not too different, one can derive from this limit a bound on the LQ–Higgs coupling,

$$Y_{LQ-\text{Higgs}} = \text{few} \cdot 10^{-6}, \tag{28}$$

for LQ masses of the order of $\mathcal{O}(200\text{ GeV})$. Such lepton number violating LQ-Higgs couplings also lead to non-zero neutrino masses at the 1-loop level [63].

4.4 Extra Dimensions

Theories with large compact extra dimensions of TeV size [64–72] have enriched dramatically the perspectives of the search for physics beyond the Standard Model. Among the possible higher-dimensional realizations, sterile neutrinos propagating in such extra dimensions [73–76] may provide interesting alternatives for generating the observed light neutrino masses. Conversely, detailed experimental studies of neutrino properties may even shed light on the geometry and shape of the new dimensions.

The minimal higher-dimensional framework of lepton number violation considers a 5-dimensional theory compactified on a S^1/Z_2 orbifold, in which only one 5-dimensional (bulk) sterile neutrino is added to the field content of the SM [77]. In this minimal model, the SM fields are localized on a 3+1-dimensional Minkowski subspace, also termed 3-brane. This model naturally generates small neutrino masses via a higher-dimensional version of the seesaw mechanism [73]. With respect to neutrinoless double beta decay an interesting feature of such extra-dimensional models is that the excitations of the sterile neutrino in the compact extra dimensions, a so-called Kaluza-Klein tower of states, contributes to the decay

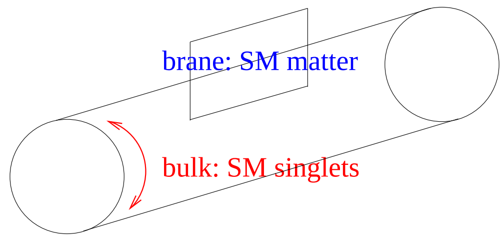

Figure 9: The SM matter is localized on a 3-brane, while the sterile singlet neutrinos are allowed to propagate in the bulk. This framework naturally generates small neutrino masses.

rate. As the masses of the exchanged Kaluza-Klein excitations range from small masses giving rise to long range contributions over the 100 MeV region up to large masses with short range contributions, such scenarios constitute a special case which is not described by the effective operator parametrization in Section 3.

Other studies on neutrinoless double beta decay were performed within the context of higher-dimensional models that assume a shining mechanism from a distant brane [78] and of theories with wrapped geometric space [79]. In the first model $0\nu\beta\beta$ decay is accompanied with the emission of Majorons [78], while the model presented in [79] predicts double beta decay at a rate being too small to be observable signal in running experiments. Another approach motivated by [74] which does not consider the effect of Kaluza-Klein states is described in [80].

The minimal higher-dimensional scenario in [77] assumes that singlet neutrinos being neutral under the $\mathrm{SU}(2)_L \otimes \mathrm{U}(1)_Y$ gauge group can freely propagate in a higher-dimensional space of $[1 + (3 + \delta)]$ dimensions, the so-called bulk, whereas all SM particles are localized on the $(3 + 1)$-dimensional brane. If the brane were located at the one of the two orbifold fixed points, the lepton number violating operators would be absent as a consequence of the Z_2 discrete symmetry. However, if the brane is shifted by an amount $a \neq 0$, these operators are no longer absent and this breaking of lepton number can lead to observable effects in neutrinoless double beta decay experiments.

One major problem of such higher-dimensional theories is their generic prediction of a KK neutrino spectrum of approximately degenerate states with opposite CP parities that lead to extremely suppressed values for the effective Majorana-neutrino mass $\langle m_\nu \rangle$. However, the KK neutrinos can couple to the W bosons with unequal strength, thus avoiding the CP-parity cancellations in the $0\nu\beta\beta$-decay amplitude. The brane-shifting parameter a can then be determined from the requirement that the effective Majorana mass $\langle m_\nu \rangle$ is in the observable range. To achieve this, $1/a$ has to be constrained to be larger than the typical Fermi nuclear momentum $q_F = 100$ MeV and much smaller than the quantum gravity scale M_F, or equivalently $1/M_F \ll a \lesssim 1/q_F$.

The masses of the Kaluza-Klein states are obtained then by diagonalizing the infinitely dimensional Kaluza-Klein mass matrix and result approximately as

$$m_{(n)} \;\approx\; \frac{n}{R} \;+\; \varepsilon\,, \tag{29}$$

where n is the index denoting the Kaluza-Klein excitation, R is the radius of the extra dimension and ε is the smallest diagonal entry in the neutrino mass matrix. The mixing-matrix elements $B_{e\nu}$ and $B_{e,n}$ follow then as [73]:

$$B_{e\nu} = \frac{1}{1+\pi^2 m^2 R^2 + \frac{m_\nu^2}{m^2}}, \quad B_{e,n} \simeq \frac{m^2\cos^2(\,\frac{na}{R} - \phi_h\,)}{(\,\frac{n}{R}+\varepsilon\,)^2}, \tag{30}$$

where a is the brane shift parameter and ϕ_h is a function of a, R and the Yukawa couplings. The $0\nu\beta\beta$-decay amplitude $\mathcal{T}_{0\nu\beta\beta}$ results as

$$\mathcal{T}_{0\nu\beta\beta} \;=\; \frac{\langle m_\nu\rangle}{m_e}\,\mathcal{M}_{\rm GTF}(m_\nu)\,, \tag{31}$$

where the combination of nuclear matrix elements $\mathcal{M}_{\rm GTF} = \mathcal{M}_{\rm GT} - \mathcal{M}_{\rm F}$ sensitively depends on the mass of the exchanged KK neutrino. As soon as the exchanged KK-neutrino mass $m_{(n)}$ is comparable or larger than the characteristic Fermi nuclear momentum $q_F \approx$ 100 MeV, the nuclear matrix element $\mathcal{M}_{\rm GTF}$ decreases as $1/m^2_{(n)}$. The general expression for the effective Majorana-neutrino mass $\langle m_\nu\rangle$ in eq. (31) is given by

$$\langle m_\nu\rangle \;=\; \frac{1}{\mathcal{M}_{\rm GTF}(m_\nu)}\,\sum_{n=-\infty}^{\infty} B^2_{e,n}\,m_{(n)}\Big[\,\mathcal{M}_{\rm GTF}(m_{(n)}) \;-\; \mathcal{M}_{\rm GTF}(m_\nu)\Big]\,. \tag{32}$$

Here the first term describes the genuine higher-dimensional effect of KK-neutrino exchanges, while the second term is the standard contribution of the light neutrino ν. The dependence of the nuclear matrix element $\mathcal{M}_{\rm GTF}$ on the KK-neutrino masses $m_{(n)}$ here has been included in the double beta observable $\langle m_\nu\rangle$. This leads to predictions for $\langle m_\nu\rangle$ that depend on the double beta emitter isotope used in the experiment. However, the difference in the predictions is typically too small to work as a smoking gun for the extra-dimensional mechanism of $0\nu\beta\beta$ decay. A particularly interesting property of this model is that the effective Majorana-neutrino mass $\langle m_\nu\rangle$ is not bounded from above by the mass eigenvalues of the light neutrinos: It can be close to the experimental limit even for an infinitesimal lightest neutrino mass m_{ν_1} which constitutes a rather unique feature of such higher-dimensional brane-shifted scenarios.

4.5 Majorons

In many theories beyond the Standard model in addition to the neutrinoless double beta decay with two electrons in the final state and nothing else, lepton number violating decay modes can arise where new scalar [81–83] or even vector particles [84] are emitted as well:

$$2n \to 2p + 2e^- + \phi, 2n \to 2p + 2e^- + 2\phi. \tag{33}$$

Majorons have been originally introduced as Nambu-Goldstone bosons being responsible for breaking a global lepton symmetry and generating neutrino Majorana masses [85, 86]. However, since such classical Majorons require severe fine-tuning in order to respect the bounds on neutrino masses and at the same time induce an observable rate for neutrinoless double beta decay, several new models have been proposed in which the term Majoron refers more broadly to a light or massless boson with couplings to neutrinos. In comparison to neutrinoless double beta decay with two electrons in the final state only, these decay modes lead to continuous spectra for the emitted electrons which can be discriminated from the Standard Model $2\nu\beta\beta$ decay by fitting the spectral shape. While expected decay rates are rather small due to suppressed nuclear matrix elements [87] experimental bounds from the Heidelberg-Moscow experiment using ^{76}Ge on various models have been derived in [88]. More recently, the NEMO-3 [89] and KAMLAND-Zen [90] collaborations have published improved bounds on these modes, constraining the Majoron-neutrino coupling constant from measurements in ^{100}Mo, ^{82}Se and ^{136}Xe e.g. for classical models to $\langle g_{ee}\rangle < (0.4 - 1.9) \cdot 10^{-4}$, $\langle g_{ee}\rangle < (0.66 - 1.7) \cdot 10^{-4}$, and $\langle g_{ee}\rangle < (0.8 - 1.6) \cdot 10^{-5}$, respectively, depending on the value of the nuclear matrix element used. For classical Majorons it has been shown in [91] that by combining bounds from next-generation double beta experiments with constraints derived from supernova energy release arguments [92] neutrino-Majoron couplings could be constrained down to a level of 10^{-7}.

4.6 Non-Standard Neutrinos

Non-standard neutrinos can contribute to neutrinoless double beta decay either as new flavours in addition to three partners of the charged leptons included in the Standard Model, or via non-standard properties or interactions.

Additional flavours have to be either sterile or heavier than half the mass of th Z boson in order to comply with the width of the Z boson. They will contribute to neutrinoless double beta decay via mixing with the electron flavour neutrino (compare the discussion in the contribution of Rodejohann). An update on a heavy 4th generation's neutrino to neutrinoless double beta decay is given in [93]. It implies that such heavy active neutrinos have to be pseudo-Dirac neutrinos with only a tiny amount of lepton number violation. The amount of lepton number violation is further constrained due to wash-out effects such weak scale pseudo-Dirac neutrinos will have on any pre-existing baryon asymmetry [94].

In principle the neutrino can also be a composite object. In this case a bound on the compositeness scale can be obtained from the neutrinoless double beta decay half life limit evaluated in the mass mechanism [95–97].

In [98] it has been discussed that observable double beta decay rates in extra-dimensional spacetimes could be triggered by the lepton number violation induced by virtual black holes violating the associated global symmetry. A somewhat related mechanism arises in theories with a saturated black hole bound on a large number of species. Such theories have been advocated recently as a possible solution to the hierarchy problem and as an explanation of the smallness of neutrino masses [99]. Then the violation of lepton number can create a potential phenomenological problem of such N-copy extensions of the Standard Model as again due to the lowered quantum gravity scale black holes may induce TeV scale LNV operators generating unacceptably large rates of e.g. neutrinoless double beta decay. It has been shown, however, that this does not happen in such a scenario due to a specific compensation mechanism between contributions of different Majorana neutrino states to these processes. As a result rates of LNV processes are extremely small and far beyond experimental reach, at least for the left-handed neutrino states [100].

Lorentz invariance and the equivalence principle are the most important pillars of special and general relativity. However, certain versions of string theories allow for or even predict the violation of these laws. Often a violation of Lorentz invariance (VLI) implies that different particles can have characteristic maximal attainable velocities. The difference of the velocities δv then parametrizes the size of VLI. Similarly, the corresponding observable describing violations of the equivalence principle (VEP) is the difference of characteristic couplings δg to the gravitational potential ϕ. While previous studies of neutrino oscillations provide very restrictive bounds in the region of large mixing [101] $0\nu\beta\beta$ decay yields in certain models of VLI and VEP a bound also in the region of zero mixing being not accessible to neutrino oscillation experiments [102]: $\delta v < 3.3 \cdot 10^{-16}$, $\phi \cdot \delta g < 3.3 \cdot 10^{-16}$. Lorentz invariance is also closely related to CPT invariance. In CPT violating models the conventional notion of Majorana neutrinos being their own anti-particles does not apply anymore. Majorana masses and double beta decay in such scenarios are discussed in [103].

5 Summary and Discussion

Neutrinoless double beta decay is a crucial observable in search for physics beyond the Standard Model as it tests the fundamental symmetry of lepton number. The violation of lepton number is predicted in many models of new physics and most prominently, it provides the only probe of the absolute mass scale of light Majorana neutrinos. In this context, searches for $0\nu\beta\beta$ are highly complementary to neutrino oscillation experiments, direct neutrino mass determinations in Tritium decay and cosmological observations of the impact of neutrinos on large scale structure formation. If the recent results at the LHC pointing to a Higgs boson with a mass of about 125 GeV are confirmed, we can expect to make a giant leap in understanding the nature of mass generation at the electroweak scale. Even then, the nature and the lightness of neutrinos would still be unexplained and so far neutrinoless double beta decay is the only realistic probe to distinguish between the Dirac or Majorana nature of light neutrinos.

As outlined in Section 3, there is large number of possible effective operators that can give rise to $0\nu\beta\beta$ decay. Only a small selection of fundamental physics models that give rise to such LNV operators were presented in Section 4. Given these ambiguities, a crucial problem is to distinguish between different mechanisms. One possibility is to compare results from $0\nu\beta\beta$ with other neutrino experiments and cosmological observations. More generally, searches for physics beyond the Standard Model at other experiments, such as the LHC, can be correlated with $0\nu\beta\beta$ in specific models. More directly, it is also possible to infer the dominant mechanism purely within the context of neutrinoless double beta decay and closely related processes. Relevant techniques discussed in the literature include (i) the comparison of $0\nu\beta\beta$ decay rates in different isotopes [104–106] (this possibility is discussed in detail in the contribution by Fogli et al.), (ii) the comparison of $0\nu\beta^-\beta^-$ with $0\nu\beta^+\beta^+$ [107], (iii) the comparison of $0\nu\beta\beta$ with electron capture [107], (iv) the comparison of of $0\nu\beta\beta$ decay to the ground state and an excited state [108] and (v) the experimental determination of the angular and energy distribution of the outgoing electrons in $0\nu\beta\beta$ [4, 109–114].

Here we highlight the potential of measuring the angular and energy distribution in $0\nu\beta\beta$ tracking experiments such as SuperNEMO [113]. Both the angular and energy correlation of the electrons depends on the effective operator mediating neutrinoless double beta decay. In the standard mass mechanism with $V-A$ couplings, the electrons are mostly emitted back to back with comparable energies. This is very different from the ϵ^{V+A}_{V+A} process shown in Fig. 4 (left), where the electrons are preferably emitted in the same direction with one electron taking away the majority of the energy. Fig. 10 shows the

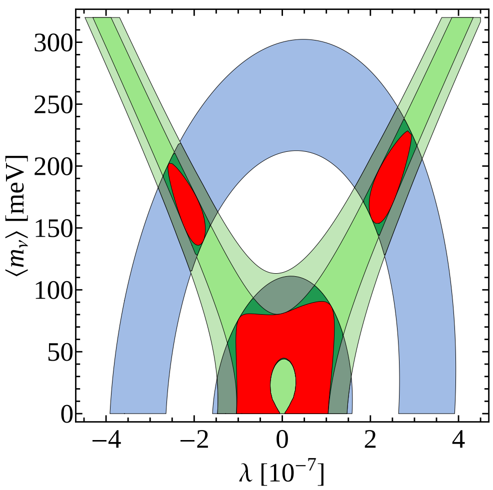

Figure 10: Simulated constraints at one standard deviation on the effective neutrino mass m_ν and LRSM coupling $\langle\lambda\rangle \equiv \epsilon^{V+A}_{V+A}$ for the isotope ^{82}Se at SuperNEMO from: (1) an observation of $0\nu\beta\beta$ decay half-life at $T_{1/2} = 10^{25}$ y (outer blue elliptical contour) and 10^{26} y (inner blue elliptical contour); (2) reconstruction of the angular (outer, lighter green) and energy difference (inner, darker green) distribution shape; (3) combination of (1) and (2) (red contours). The strength of the λ contribution is assumed to be 30% of the standard mass mechanism. NME uncertainties are assumed to be 30% and experimental statistical uncertainties are determined from the simulation in [113].

impact of combining the total $0\nu\beta\beta$ rate measurement with a determination of the angular and energy distribution shape at SuperNEMO. In the hypothetical scenario considered, both the standard mass mechanism and the operator of ϵ^{V+A}_{V+A} are assumed to contribute; whereas the total rate alone can not differentiate between the two contributions, taking into account the angular and energy shape can allow to pinpoint their relative size.

If neutrinoless double beta decay is observed in next generation experiments at a level corresponding to an effective $0\nu\beta\beta$ mass $m_{ee} \gtrsim 10^{-2}$ eV, it would be an indication that the decay is caused by the exchange of light neutrinos, especially if corroborated by cosmological observations. On the other hand, such a conclusion is not straightforward as there is a large number of models which can trigger neutrinoless double beta decay. As discussed in this article, such new physics mechanisms can be economically categorized in terms of effective Lorentz invariant operators. Due to the black box theorem [2, 3, 13], the observation of neutrinoless double beta decay will prove that the light left-handed neutrinos are Majorana particles, but from this alone it is not possible to infer the dominant operator and mechanism.

Acknowledgements

M.H. acknowledges support from the Spanish MICINN grants FPA2011-22975, MULTI-DARK CSD2009-00064 and by the Generalitat Valenciana grant Prometeo/2009/091 and the EU Network grant UNILHC PITN-GA-2009-237920.

References

[1] W. Rodejohann, 1206.2560.

[2] J. Schechter and J. Valle, Phys.Rev. **D25**, 2951 (1982).

[3] J. F. Nieves, Phys.Lett. **B147**, 375 (1984).

[4] M. Doi, T. Kotani and E. Takasugi, Prog.Theor.Phys.Suppl. **83**, 1 (1985).

[5] M. Hirsch, H. Klapdor-Kleingrothaus and O. Panella, Phys.Lett. **B374**, 7 (1996), [hep-ph/9602306].

[6] M. Hirsch, H. Klapdor-Kleingrothaus and S. Kovalenko, Phys.Rev.Lett. **75**, 17 (1995).

[7] M. Hirsch, H. Klapdor-Kleingrothaus and S. Kovalenko, Phys.Rev. **D53**, 1329 (1996), [hep-ph/9502385].

[8] K. Babu and R. Mohapatra, Phys.Rev.Lett. **75**, 2276 (1995), [hep-ph/9506354].

[9] M. Hirsch, H. Klapdor-Kleingrothaus and S. Kovalenko, Phys.Lett. **B372**, 181 (1996), [hep-ph/9512237].

[10] H. Päs, M. Hirsch and H. Klapdor-Kleingrothaus, Phys.Lett. **B459**, 450 (1999), [hep-ph/9810382].

[11] M. Hirsch, H. Klapdor-Kleingrothaus and S. Kovalenko, Phys.Lett. **B378**, 17 (1996), [hep-ph/9602305].

[12] M. Hirsch, H. Klapdor-Kleingrothaus and S. Kovalenko, Phys.Rev. **D54**, 4207 (1996), [hep-ph/9603213].

[13] E. Takasugi, Phys.Lett. **B149**, 372 (1984).

[14] M. Duerr, M. Lindner and A. Merle, JHEP **1106**, 091 (2011), [1105.0901].

[15] M. Hirsch, H. Klapdor-Kleingrothaus and S. Kovalenko, Phys.Lett. **B398**, 311 (1997), [hep-ph/9701253].

[16] M. Hirsch, H. Klapdor-Kleingrothaus and S. Kovalenko, Phys.Rev. **D57**, 1947 (1998), [hep-ph/9707207].

[17] M. Hirsch, H. Klapdor-Kleingrothaus and S. Kovalenko, Phys.Lett. **B403**, 291 (1997).

[18] Y. Grossman and H. E. Haber, Phys.Rev.Lett. **78**, 3438 (1997), [hep-ph/9702421].

[19] M. Hirsch, H. Klapdor-Kleingrothaus, S. Kolb and S. Kovalenko, Phys.Rev. **D57**, 2020 (1998).

[20] M. Hirsch, S. Kovalenko and I. Schmidt, Phys.Lett. **B642**, 106 (2006), [hep-ph/0608207].

[21] H. Päs, M. Hirsch, H. Klapdor-Kleingrothaus and S. Kovalenko, Phys.Lett. **B453**, 194 (1999).

[22] H. Päs, M. Hirsch, H. Klapdor-Kleingrothaus and S. Kovalenko, Phys.Lett. **B498**, 35 (2001), [hep-ph/0008182].

[23] G. Prezeau, M. Ramsey-Musolf and P. Vogel, Phys.Rev. **D68**, 034016 (2003), [hep-ph/0303205].

[24] H. Päs, Dissertation, Heidelberg (1999).

[25] A. Faessler, G. Fogli, E. Lisi, A. Rotunno and F. Simkovic, Phys.Rev. **D83**, 113015 (2011), [1103.2504].

[26] J. Menendez, A. Poves, E. Caurier and F. Nowacki, J.Phys.Conf.Ser. **312**, 072005 (2011).

[27] F. Simkovic, A. Faessler, V. Rodin, P. Vogel and J. Engel, Phys.Rev. **C77**, 045503 (2008), [0710.2055].

[28] M. Kortelainen and J. Suhonen, Phys.Rev. **C76**, 024315 (2007), [0708.0115].

[29] O. Civitarese and J. Suhonen, J.Phys.Conf.Ser. **173**, 012012 (2009).

[30] F. Simkovic, A. Faessler, H. Muther, V. Rodin and M. Stauf, Phys.Rev. **C79**, 055501 (2009), [0902.0331].

[31] H. Klapdor-Kleingrothaus *et al.*, Eur.Phys.J. **A12**, 147 (2001), [hep-ph/0103062].

[32] EXO Collaboration, M. Auger *et al.*, 1205.5608.

[33] H. Klapdor-Kleingrothaus, A. Dietz, H. Harney and I. Krivosheina, Mod.Phys.Lett. **A16**, 2409 (2001), [hep-ph/0201231].

[34] H. Klapdor-Kleingrothaus, I. Krivosheina, A. Dietz and O. Chkvorets, Phys.Lett. **B586**, 198 (2004), [hep-ph/0404088].

[35] H. Klapdor-Kleingrothaus and I. Krivosheina, Mod.Phys.Lett. **A21**, 1547 (2006).

[36] K. Muto, E. Bender and H. Klapdor, Z.Phys. **A334**, 187 (1989).

[37] M. Hirsch, H. Klapdor-Kleingrothaus and S. Kovalenko, Phys.Lett. **B352**, 1 (1995), [hep-ph/9502315].

[38] T. Tomoda, Rept.Prog.Phys. **54**, 53 (1991).

[39] S. L. Adler *et al.*, Phys.Rev. **D11**, 3309 (1975).

[40] J. Vergados, Phys.Rev. **C24**, 640 (1981).

[41] J. Vergados, Nucl.Phys. **B218**, 109 (1983).

[42] B. Brahmachari and E. Ma, Phys.Lett. **B536**, 259 (2002), [hep-ph/0202262].

[43] P. Fileviez Perez and M. B. Wise, Phys.Rev. **D80**, 053006 (2009), [0906.2950].

[44] S. Choubey, M. Duerr, M. Mitra and W. Rodejohann, JHEP **1205**, 017 (2012), [1201.3031].

[45] W. Rodejohann, Int.J.Mod.Phys. **E20**, 1833 (2011), [1106.1334].

[46] J. C. Pati and A. Salam, Phys.Rev. **D10**, 275 (1974).

[47] R. Mohapatra and J. C. Pati, Phys.Rev. **D11**, 2558 (1975).

[48] G. Senjanovic and R. N. Mohapatra, Phys.Rev. **D12**, 1502 (1975).

[49] P. Duka, J. Gluza and M. Zralek, Annals Phys. **280**, 336 (2000), [hep-ph/9910279].

[50] J. Schechter and J. Valle, Phys.Rev. **D25**, 774 (1982).

[51] S. Das, F. Deppisch, O. Kittel and J. Valle, 1206.0256.

[52] ATLAS Collaboration, G. Aad *et al.*, 1203.5420, 9 pages plus author list (23 pages total), 4 figures, 3 tables, submitted to European Physical Journal C.

[53] H. K. Dreiner, hep-ph/9707435.

[54] M. Hirsch and J. Valle, New J.Phys. **6**, 76 (2004), [hep-ph/0405015].

[55] A. Balysh *et al.*, Phys.Lett. **B356**, 450 (1995).

[56] B. Allanach, C. Kom and H. Päs, Phys.Rev.Lett. **103**, 091801 (2009), [0902.4697].

[57] B. Allanach, C. Kom and H. Päs, JHEP **0910**, 026 (2009), [0903.0347].

[58] S. Dimopoulos and L. J. Hall, Phys.Lett. **B207**, 210 (1988).

[59] H. K. Dreiner, P. Richardson and M. H. Seymour, Phys.Rev. **D63**, 055008 (2001), [hep-ph/0007228].

[60] W. Buchmüller, R. Rückl and D. Wyler, Phys.Lett. **B191**, 442 (1987).

[61] S. Davidson, D. C. Bailey and B. A. Campbell, Z.Phys. **C61**, 613 (1994), [hep-ph/9309310].

[62] Particle Data Group, K. Nakamura *et al.*, J.Phys.G **G37**, 075021 (2010).

[63] D. Aristizabal Sierra, M. Hirsch and S. Kovalenko, Phys.Rev. **D77**, 055011 (2008), [0710.5699].

[64] N. Arkani-Hamed, S. Dimopoulos and G. Dvali, Phys.Lett. **B429**, 263 (1998), [hep-ph/9803315].

[65] I. Antoniadis, N. Arkani-Hamed, S. Dimopoulos and G. Dvali, Phys.Lett. **B436**, 257 (1998), [hep-ph/9804398].

[66] K. R. Dienes, E. Dudas and T. Gherghetta, Phys.Lett. **B436**, 55 (1998), [hep-ph/9803466].

[67] K. R. Dienes, E. Dudas and T. Gherghetta, Nucl.Phys. **B537**, 47 (1999), [hep-ph/9806292].

[68] L. Randall and R. Sundrum, Phys.Rev.Lett. **83**, 3370 (1999), [hep-ph/9905221].

[69] I. Antoniadis, Phys.Lett. **B246**, 377 (1990).

[70] J. D. Lykken, Phys.Rev. **D54**, 3693 (1996), [hep-th/9603133].

[71] P. Horava and E. Witten, Nucl.Phys. **B460**, 506 (1996), [hep-th/9510209].

[72] P. Horava and E. Witten, Nucl.Phys. **B475**, 94 (1996), [hep-th/9603142].

[73] K. R. Dienes, E. Dudas and T. Gherghetta, Nucl.Phys. **B557**, 25 (1999), [hep-ph/9811428].

[74] N. Arkani-Hamed, S. Dimopoulos, G. Dvali and J. March-Russell, Phys.Rev. **D65**, 024032 (2002), [hep-ph/9811448].

[75] A. Pilaftsis, Phys.Rev. **D60**, 105023 (1999), [hep-ph/9906265].

[76] A. Ioannisian and A. Pilaftsis, Phys.Rev. **D62**, 066001 (2000), [hep-ph/9907522].

[77] G. Bhattacharyya, H. Klapdor-Kleingrothaus, H. Päs and A. Pilaftsis, Phys.Rev. **D67**, 113001 (2003), [hep-ph/0212169].

[78] R. Mohapatra, A. Perez-Lorenzana and C. de S Pires, Phys.Lett. **B491**, 143 (2000), [hep-ph/0008158].

[79] S. J. Huber and Q. Shafi, Phys.Lett. **B544**, 295 (2002), [hep-ph/0205327].

[80] M. Gozdz, W. A. Kaminski, F. Simkovic and A. Faessler, Phys.Rev. **D74**, 055007 (2006), [hep-ph/0606077].

[81] C. Burgess and J. M. Cline, Phys.Lett. **B298**, 141 (1993), [hep-ph/9209299].

[82] C. Burgess and J. M. Cline, Phys.Rev. **D49**, 5925 (1994), [hep-ph/9307316].

[83] P. Bamert, C. Burgess and R. Mohapatra, Nucl.Phys. **B449**, 25 (1995), [hep-ph/9412365].

[84] C. D. Carone, Phys.Lett. **B308**, 85 (1993), [hep-ph/9302290].

[85] Y. Chikashige, R. N. Mohapatra and R. Peccei, Phys.Lett. **B98**, 265 (1981).

[86] G. Gelmini and M. Roncadelli, Phys.Lett. **B99**, 411 (1981).

[87] M. Hirsch, H. Klapdor-Kleingrothaus, S. Kovalenko and H. Päs, Phys.Lett. **B372**, 8 (1996), [hep-ph/9511227].

[88] Heidelberg - Moscow-Collaboration, J. Bockholt *et al.*, Phys.Rev. **D54**, 3641 (1996), [nucl-ex/9511001].

[89] NEMO Collaboration, R. Arnold *et al.*, Nucl.Phys. **A765**, 483 (2006), [hep-ex/0601021].

[90] KamLAND-Zen Collaboration, A. Gando *et al.*, 1205.6372.

[91] R. Tomas, H. Päs and J. Valle, Phys.Rev. **D64**, 095005 (2001), [hep-ph/0103017].

[92] M. Kachelriess, R. Tomas and J. Valle, Phys.Rev. **D62**, 023004 (2000), [hep-ph/0001039].

[93] A. Lenz, H. Päs and D. Schalla, Phys.Rev. **D85**, 075025 (2012), [1104.2465].

[94] S. Hollenberg, H. Päs and D. Schalla, 1110.0948.

[95] E. Takasugi, Prog.Theor.Phys. **94**, 1097 (1995), [hep-ph/9506379].

[96] E. Takasugi, Prog.Theor.Phys. **98**, 977 (1997), [hep-ph/9706240].

[97] O. Panella, C. Carimalo, Y. Srivastava and A. Widom, Phys.Rev. **D56**, 5766 (1997), [hep-ph/9701251].

[98] Y. Uehara, hep-ph/0205294.
[99] G. Dvali and M. Redi, Phys.Rev. **D80**, 055001 (2009), [0905.1709].
[100] S. Kovalenko, H. Päs and I. Schmidt, J.Phys.Conf.Ser. **259**, 012070 (2010), [1011.0410].
[101] C. N. Leung, Nucl.Instrum.Meth. **A451**, 81 (2000), [hep-ph/0002073].
[102] H. Klapdor-Kleingrothaus, H. Päs and U. Sarkar, Eur.Phys.J. **A5**, 3 (1999), [hep-ph/9809396].
[103] G. Barenboim, J. F. Beacom, L. Borissov and B. Kayser, Phys.Lett. **B537**, 227 (2002), [hep-ph/0203261].
[104] S. Bilenky and S. Petcov, hep-ph/0405237.
[105] F. Deppisch and H. Päs, Phys.Rev.Lett. **98**, 232501 (2007), [hep-ph/0612165].
[106] V. Gehman and S. Elliott, J.Phys.G **G34**, 667 (2007), [hep-ph/0701099].
[107] M. Hirsch, K. Muto, T. Oda and H. Klapdor-Kleingrothaus, Z.Phys. **A347**, 151 (1994).
[108] F. Simkovic, M. Nowak, W. Kaminski, A. Raduta and A. Faessler, Phys.Rev. **C64**, 035501 (2001), [nucl-th/0107016].
[109] M. Doi, T. Kotani, H. Nishiura and E. Takasugi, Prog.Theor.Phys. **69**, 602 (1983).
[110] T. Tomoda, A. Faessler, K. Schmid and F. Grummer, Nucl.Phys. **A452**, 591 (1986).
[111] A. Ali, A. Borisov and D. Zhuridov, hep-ph/0606072.
[112] A. Ali, A. Borisov and D. Zhuridov, Phys.Rev. **D76**, 093009 (2007), [0706.4165].
[113] SuperNEMO Collaboration, R. Arnold *et al.*, Eur.Phys.J. **C70**, 927 (2010), [1005.1241].
[114] F. Deppisch, C. Jackson, I. Nasteva and S. Soldner-Rembold, Prog.Part.Nucl.Phys. **64**, 278 (2010).